

WAVE OVERWASH AT LOW-CRESTED BEACH BARRIERS

THIEU QUANG TUAN¹

Email address: T.Thieuquang@tudelft.nl , Tuan.t.q@wru.edu.vn

HENK JAN VERHAGEN²

Email address: H.J.Verhagen@.tudelft.nl

PAUL VISSER²

Email address: P.J.Visser@tudelft.nl

MARCEL J.F. STIVE²

Email address: M.J.F.Stive@.tudelft.nl

¹ *Faculty of Coastal Engineering*

Water Resources University (WRU)

175 Tay Son, Dong Da District, Hanoi, Vietnam

Research fellow at Section of Hydraulic Engineering, Delft University of Technology,

The Netherlands.

² *Section of Hydraulic Engineering*

Faculty of Civil Engineering and Geosciences

Delft University of Technology (DUT)

Stevinweg 1

P.O. Box 5048, 2600 GA Delft, The Netherlands.

Abstract

To increase physical insight into wave overwash processes at low-crested beach barriers, wave overtopping discharge events rather than the conventional average overtopping discharge need to be quantified. Also, in order to make intelligent use of the many empirical formulations on wave overtopping discharge at breakwaters from literature, a single-valued appropriate slope for a natural beach needs to be derived. To resolve these issues, laboratory experiments of composite-slope low-crested barriers were carried out. The tests deal with overwash on a smooth non-uniform slope on shallow foreshores.

The conventional average overtopping discharge concept does not represent the discontinuous character and associated strength of overtopping flow. Instead, e.g. for purposes of morphological modeling, wave overtopping should be treated as an event-based process. In this study, several new parameters such as the wave-averaged overtopping time, the relative total overtopping time, the overtopping asymmetry, the average maximum discharge and the average instantaneous discharge are defined and formulated.

A new approach for defining an equivalent slope is proposed in the parameterization of the overtopping discharge that also takes into account effects of the wave period. It is experimentally shown to be an improvement over the conventional approach by Van der Meer [1998], especially eligible for low-crested sandy slopes such as barriers, dikes, dunes, etc. on shallow foreshores.

Keywords

Equivalent slope, low-crested, shallow foreshores, overwash, event-based, wave overtopping.

1 Introduction

Wave overwash during severe storms can induce breakthroughs of coastal barriers at depressed sections, probably causing losses of human lives and properties and damages to infrastructures (see e.g. Latherman, 1981). Quantitative understanding of wave overwash is therefore of crucial engineering interest to improve model predictions for beach and dune erosion and especially coastal flooding hazards during storms.

Numerical modeling of wave overwash relies heavily on the prediction of overtopping parameters as the requisite hydraulic input at the entrance crest boundary (see problem schematization in Fig. 1).

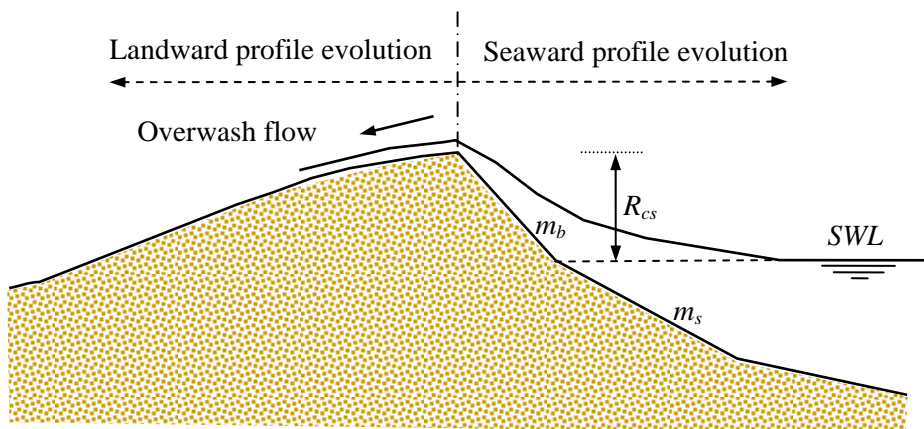


Figure 1. Wave overtopping as the hydraulic input for overwash modeling.

As a starting point we adopt overtopping discharge formulations from breakwater literature. Most of these formulations have been developed for laboratory conditions where uniform slopes were used. On natural beaches, the profile is more very complex and thus an appropriate equivalent slope for use in those predictive formulae is not straightforward. Different slope definitions can lead to substantial differences in overtopping estimates.

Kobayashi *et al.* [1996] carried out tests on overwash of dunes and compare overtopping rates with the existing formulations of Van der Meer *et al.* [1995], which were originally developed for hard slope coastal structures. An equivalent uniform slope also according to Van der Meer *et al.* [1995] was used. These formulae were found to predict only the order of magnitude of the measured overtopping rates. The study reveals that the accuracy of overtopping estimates is

relatively sensitive to the magnitude of the calculated equivalent slope. The adaptation of the uniform equivalent slope concept from a hard slope to a sandy beach is therefore an issue to be further considered.

Prediction of runup on sandy beaches encounters a similar problem. Mayer and Kriebel [1994] combined the Hunt runup formula and Saville's hypothetical slope concept to provide first-order estimates of wave runup over composite slope beaches. Improvements over the existing formulae were found and attributed to proper adjustment of the beach slope. However, the finding is rather an ad hoc modification of wave runup formulae than a direct improvement on the equivalent slope for sandy beaches.

Tuan [2003] investigated from literature the characteristics of dune profile development during storms. It was noted that short-term evolution of sandy profiles can be well distinguished into two parts i.e. above (dry beach) and below (submerged beach) the still water line. Based on this notion, the author proposed a general form of the equivalent slope that can be used in the calculation of wave overtopping discharge, using existing empirical formulations.

Based on the findings of Kobayashi *et al.* [1996], Tega and Kobayashi [1999] performed a numerical study on dune evolution due to wave overwash. The model failed to reproduce the measured dune profiles satisfactorily. This was, in part, due to the use of the conventional average overtopping discharge, which is too simplistic in this case. It was recommended to seek for a better description of wave overtopping.

In general, discharge due to wave overtopping is discontinuous and concentrates in durations less than one wave period. The average discharge is therefore unsuitable to characterize the discontinuous character of overtopping. Instead, e.g. for purposes of morphological modeling, wave overtopping should be treated as an event-based process, and this process should be characterized by a new set of descriptive parameters.

In pursuit of this, an experimental investigation of wave overtopping at composite slope barriers on shallow foreshores was carried out. Low-crested conditions associated with moderate to severe overtopping were selected for the tests. The experimental data are used to formulate

event-based wave overtopping discharge under the assumption of form similarity between individual events, i.e. parameterizing its time-dependent properties over the wave cycle, neglecting unsteady effects caused by previous waves. The newly-defined parameters are the wave-averaged overtopping time, the relative total overtopping time, the overtopping asymmetry, and the average instantaneous discharge. Previous work of Tuan [2003] on a new slope definition has also been extended and calibrated.

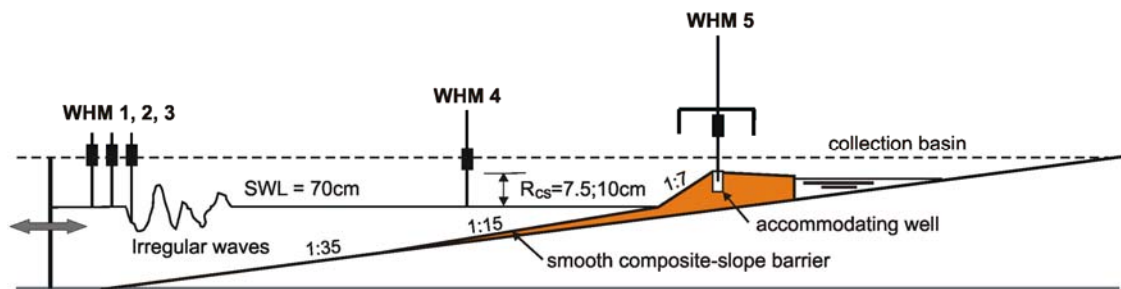


Figure 2. Experimental setup of overtopping tests

2 Experimental setup

A scale model was constructed in the 40m long wave flume at the laboratory of Delft University of Technology. The wave maker, which is equipped with Active Reflection Compensation, is capable of generating regular and irregular waves up to 25cm.

The experimental setup consisted of impermeable model barriers on a 1/35 sloping foreshore with two different crest freeboards and slope compositions (see Fig.2 and Table 1). These slopes were made smooth securing a roughness reduction to achieve a proper scaling for wave overtopping. The initial water level in the flume was always related to the transition point of the barrier slope at the depth of 0.70 m.

Five wave height meters (WHM) were placed at various locations along the flume. WHM1-3 and WHM4 were used for the decomposition of the incident and reflected waves at the seaward most boundary and at the toe of the barrier.

Since wave by wave overtopping is of crucial interest, WHM5 was installed on the barrier crest. Since a minimum water depth of 5cm is always required, WHM5 is accommodated with a well

of 10cm deep (see Fig. 3). In order to sense the presence of water even with minor disturbances, this gauge was set to a range of high sensitivity.



Figure 3. On-crest accommodation well for the overtopping gauge.

Random waves with standard JONSWAP-shaped spectra were employed in the experiment. Test parameters were chosen in such a way that the wave heights H_{mo} at the toe of the barrier are larger than the crest freeboards R_{cs} (or the ratio $R_{cs}/H_{mo} \leq 1$), which corresponds to the condition of moderate to heavy wave overtopping. This resulted in a test program consisting of 35 tests with parameters specified in Table 1.

3 Analysis of experimental results

Since there was no means of disturbance-free supply of water back into the flume, the mean water level was slowly falling during the measurement. This means in fact that the crest freeboard was slowly increasing, depending on the severity of overtopping. To account for this effect, an averaged crest freeboard is determined for each test as follows:

$$R_{cs} = R_{cs0} + \frac{1}{2} \Delta R_{cs}. \quad (1)$$

In which R_{cs0} is the initial (before test) crest freeboard (10 or 7.5 cm), ΔR_{cs} is the total level fall (at the end of a test) relative to the initial level. On the whole, the maximum fall of the water level was about 2cm, implying 1cm of additional increase of freeboard for the heaviest overtopping (see Eq. 1).

In principle, the falling process of the mean water level during a test will influence the waves. Control tests (without overtopping) with a difference in the mean flume level of 1cm showed minor variations in the measured wave heights (< 1% at the wave-board section and <5% at the

Table 1. Experimental conditions of 35 overtopping tests.

Test run	T	$H_{m0,i}$	T_P	S_{op}	$T_{m-1.0, toe}$	$H_{m0,toe}$	$\frac{R_{cs}}{H_{m0,toe}}$	$\xi_{m,toe}$	$\frac{H_{m0,i}}{d_{toe}}$
	(min.)	(m)	(sec.)	(-)	(sec.)	(m)	(-)	(-)	(-)
Crest freeboard $R_{cs} = 7.5$ cm $m_s = 0.064$ $m_b = 0.138$									
1	30	0.123	1.50	0.035	1.36	0.098	0.82	0.35 ~ 0.75 (0.45)	1.30
2	30	0.139	1.50	0.040	1.40	0.101	0.80	0.35 ~ 0.76 (0.45)	1.15
3	36	0.106	1.70	0.024	1.41	0.097	0.83	0.36 ~ 0.78 (0.47)	1.51
4	36	0.125	1.70	0.028	1.44	0.102	0.80	0.36 ~ 0.78 (0.46)	1.28
5	36	0.142	1.70	0.031	1.49	0.104	0.80	0.37 ~ 0.80 (0.47)	1.13
6	40	0.107	2.00	0.017	1.51	0.100	0.82	0.38 ~ 0.82 (0.49)	1.50
7	40	0.126	2.00	0.020	1.57	0.104	0.81	0.39 ~ 0.84 (0.50)	1.27
8	40	0.144	2.00	0.023	1.67	0.106	0.82	0.41 ~ 0.88 (0.52)	1.11
9	40	0.163	2.00	0.026	1.77	0.107	0.82	0.43 ~ 0.93 (0.55)	0.98
10	42	0.107	2.30	0.013	1.62	0.101	0.84	0.41 ~ 0.88 (0.52)	1.50
11	42	0.127	2.30	0.015	1.71	0.106	0.82	0.42 ~ 0.91 (0.54)	1.26
12	42	0.146	2.30	0.018	1.84	0.107	0.84	0.45 ~ 0.97 (0.57)	1.10
13	42	0.165	2.30	0.020	1.96	0.109	0.83	0.47 ~ 1.02 (0.60)	0.97
14	45	0.108	2.50	0.011	1.68	0.102	0.84	0.42 ~ 0.91 (0.54)	1.48
15	48	0.127	2.50	0.013	1.80	0.106	0.84	0.44 ~ 0.95 (0.56)	1.26
16	45	0.147	2.50	0.015	1.94	0.108	0.84	0.47 ~ 1.02 (0.60)	1.09
17	50	0.108	2.70	0.009	1.75	0.102	0.86	0.44 ~ 0.94 (0.56)	1.48
18	50	0.127	2.70	0.011	1.89	0.106	0.86	0.46 ~ 1.00 (0.59)	1.26
Crest freeboard $R_{cs} = 10$ cm $m_s = 0.064$ $m_b = 0.125$									
1	30	0.142	1.50	0.040	1.39	0.104	0.97	0.34 ~ 0.67 (0.45)	1.13
2	30	0.158	1.50	0.045	1.44	0.106	0.96	0.35 ~ 0.69 (0.46)	1.01
3	35	0.127	1.70	0.028	1.43	0.104	0.97	0.35 ~ 0.69 (0.46)	1.26
4	35	0.145	1.70	0.032	1.48	0.107	0.95	0.36 ~ 0.71 (0.47)	1.10
5	35	0.163	1.70	0.036	1.54	0.108	0.95	0.37 ~ 0.73 (0.49)	0.98
6	40	0.118	2.00	0.019	1.54	0.105	0.97	0.38 ~ 0.74 (0.50)	1.36
7	40	0.146	2.00	0.023	1.65	0.109	0.96	0.40 ~ 0.78 (0.52)	1.10
8	40	0.164	2.00	0.026	1.74	0.109	0.97	0.42 ~ 0.82 (0.55)	0.98
9	40	0.128	2.30	0.016	1.69	0.108	0.96	0.41 ~ 0.80 (0.54)	1.25
10	40	0.148	2.30	0.018	1.79	0.111	0.96	0.43 ~ 0.84 (0.56)	1.08
11	40	0.168	2.30	0.020	1.89	0.112	0.96	0.45 ~ 0.88 (0.59)	0.95
12	45	0.110	2.50	0.011	1.66	0.101	1.00	0.42 ~ 0.82 (0.55)	1.45
13	46	0.129	2.50	0.013	1.77	0.106	0.99	0.43 ~ 0.85 (0.57)	1.24
14	45	0.158	2.50	0.016	1.96	0.110	0.99	0.47 ~ 0.92 (0.62)	1.01
15	45	0.140	2.50	0.014	1.83	0.110	0.97	0.44 ~ 0.86 (0.58)	1.14
16	50	0.139	2.70	0.012	1.92	0.112	0.97	0.46 ~ 0.90 (0.60)	1.15
17	50	0.160	2.70	0.014	2.07	0.113	0.98	0.49 ~ 0.96 (0.64)	1.00

Note: Variations of the surf similarity parameter $\xi_{m,toe}$ are associated with the tuning range $\eta = 0 \sim 1$. Values in brackets are based on the conventional approach by Van der Meer [1998].

toe section). Furthermore, the level fall effects are actually taken into consideration in the current analysis, explicitly via the use of the test-averaged water level (Eq. 1) and implicitly in

the measured wave heights themselves. Within the above range of the flume drawdown, its effects on the overtopping parameterization are therefore negligibly small.

3.1 Wave reflection

As mentioned earlier, three gauges located at the horizontal portion of the flume before the slope were used to decompose incident and reflected waves. In general, reflected waves were rather small in all tests, owing to the ARC of the wave generator and the mildness of the foreshore slope. The overall reflection coefficient C_r , defined in Eq. (2) below, varied between 1~5 %.

$$C_r = \sqrt{\frac{m_{0,r}}{m_{0,i}}} \quad (2)$$

Where $m_{0,i}$ and $m_{0,r}$ are the zeroth spectral moments of incident and reflected waves, respectively.

3.2 Signal of wave overtopping

In Fig. 4 the disturbance of overtopping waves displayed in volts on the vertical axis is clearly discriminated by discontinuous asymmetric triangles. However, there exists noise between these peaks, which was in fact caused by water level fluctuation within the accommodation well. In order to eliminate this noise and obtain the information needed on each individual overtopping wave, an algorithm of “local threshold” was applied. Any arbitrary reading, which has a signal value larger than its local threshold, is recognized as a registration of an overtopping event. This threshold is determined locally between each pair of overtopping triangles as follows:

$$A_{thres} = \bar{A} + a_{fluct} \quad (3)$$

Where A_{thres} is a local threshold, \bar{A} is the averaged signal value between two considered peaks, a_{fluct} is the fluctuation margin.

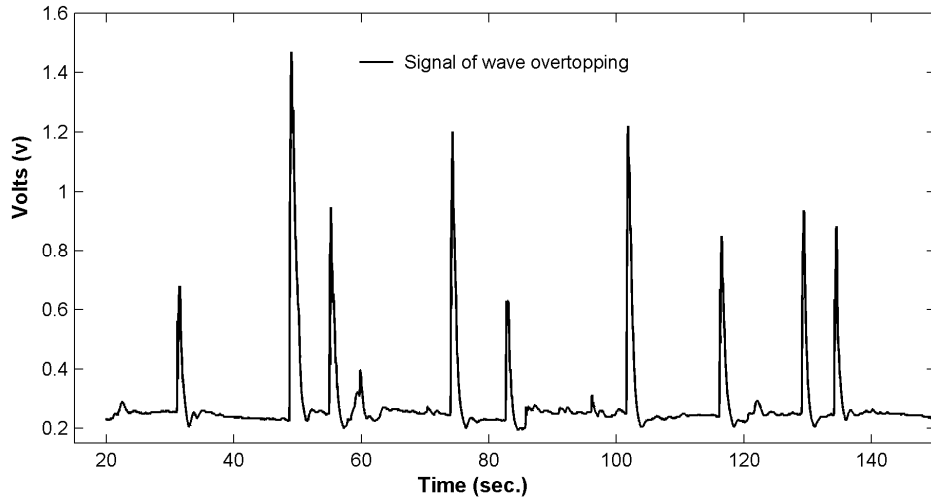


Figure 4. A sample of wave overtopping signal.

The value of a_{fluct} in Eq. (3) was determined by testing the gauge (WHM5) with fluctuating water within the well. This method was also verified against visual observations on the number of overtopping waves in several calibration tests.

The layer thickness of the overtopping flow is very small (of the order of a centimeter). Moreover, the effect of wave rise against the gauge on the overtopping signals is somewhat erratic.

Therefore, although the signal output from this gauge matched well with our visual observations, we concluded that the quantitative values of the layer thickness are unreliable, but that the duration and the instant of maximum discharge of the overwash event are reliable.

3.3 Description of overtopping key parameters

As mentioned earlier, it is desired to improve the description of wave overtopping that can be used for various modeling purposes. In the current study, the ultimate goal is to formulate the instantaneous (time-varying) discharge of the overwash event in terms of the barrier geometry and incident hydraulic conditions. The following parameters that were directly or indirectly measured during the experiment are thus proposed in the elaboration.

Average overtopping discharge q ($m^3/s/m$)

This discharge quantity is widely used in coastal engineering designs. It is averaged over the entire test (or storm) duration T .

$$q = \frac{V_{ovt}}{T}. \quad (4)$$

Where V_{ovt} is the total overtopping volume.

Number of overtopping waves N_{ovt} .

This number is counted using the algorithm of local threshold mentioned earlier.

Total overtopping time T_{ovt} (sec.)

T_{ovt} is determined as the summation of overtopping time of all individual waves that pass the barrier crest.

$$T_{ovt} = \sum_1^{N_{ovt}} t_{ovt,w}. \quad (5)$$

Where $t_{ovt,w}$ is the overtopping time of an individual overtopped wave.

Relative total overtopping time F_{cd}

Wave overtopping is discontinuous and condensed to time durations less than one wave period.

The relative total overtopping time is therefore defined according to:

$$F_{cd} = \frac{T_{ovt}}{T} = \frac{\sum_1^{N_{ovt}} t_{ovt,w}}{T}. \quad (6)$$

This parameter represents the discontinuous character of overtopping, viz. the smaller F_{cd} the more discontinuous overtopping and vice versa. By definition, F_{cd} is smaller than unity ($F_{cd} < 1$).

Wave-averaged overtopping time t_{ovt} (sec.)

This quantity is the average overtopping time per wave according to:

$$t_{ovt} = \frac{T_{ovt}}{N_w} = F_{cd} T_m. \quad (7)$$

Where T_m is a characteristic wave period. N_w is the characteristic number of waves determined according to T_m , $N_w = T/T_m$.

Overtopping Asymmetry

Overtopping peaks as seen in Fig. 4 are appreciably similar in shape. This form similarity can be characterized by an overall asymmetric factor which is defined as the ratio of the total rising time to the total overtopping time of all overtopped waves (see also Fig. 5).

$$\delta = \frac{\sum_1^{N_{ovt}} t_{rise,w}}{T_{ovt}} = \frac{\sum_1^{N_{ovt}} t_{rise,w}}{\sum_1^{N_{ovt}} t_{ovt,w}} = \frac{t_{rise}}{t_{ovt}} < 1. \quad (8)$$

Where δ is the asymmetric factor; t_{rise} is the total rising time of overtopping waves; the subscript $(.)_w$ denotes an individual wave value.

Average instantaneous discharge and average maximum discharge

The triangular shapes in the overtopping signal as shown in Fig. 4 suggest the existence of a dominating peak discharge in each overtopping wave. We argue that the data are not accurate enough to characterize individual overtopping events. As a first-order approximation we suggest to adopt an average instantaneous discharge schematization based on an asymmetric triangular shape (see Fig. 5), constrained by the total overtopping volume. Inaccuracies in the triangular shape assumption will not affect the results in a relative sense and only marginally in absolute sense.

Hence, the average maximum discharge can be derived based on the property of mass conservation:

$$\text{Mass conservation: } \frac{1}{2} q_{cd \max} t_{ovt} N_{waves} = qT = V_{ovt}.$$

Substituting $T_{ovt} = t_{ovt} N_{waves}$ in the above equation yields: $\frac{1}{2} q_{cd\max} T_{ovt} = qT$.

Finally we have:

$$q_{cd\max} = 2 \frac{q}{F_{cd}}. \quad (9)$$

The triangular discharge histogram (Fig. 5) or the average instantaneous discharge can be expressed as functions of time as follows:

$$\frac{q_{cd}(t)}{q_{cd\max}} = \frac{1}{\delta} \frac{t}{t_{ovt}} \quad \text{with } 0 \leq t \leq \delta t_{ovt}. \quad (10)$$

$$\frac{q_{cd}(t)}{q_{cd\max}} = \frac{1}{1-\delta} \left(1 - \frac{t}{t_{ovt}} \right) \quad \text{with } \delta t_{ovt} < t \leq t_{ovt}. \quad (11)$$

$$q_{cd}(t) = 0 \quad \text{with } t_{ovt} < t \leq T_m. \quad (12)$$

Where $q_{cd}(t)$ and $q_{cd\max}$ are the average instantaneous discharge and its maximum, respectively.

The average instantaneous discharge is one step forward in characterizing the intense, discontinuous temporal variation of wave overtopping. In the current research context, it is used to specify the event-averaged wave-cycle input discharges at the upstream boundary in the numerical modeling of wave overwash. In a broader sense, this event-based description of the discharge is conceptually adaptable to other coastal research issues such as on structural stability and erosion induced by overtopping flow where the use of the conventional average discharge might be inadequate. An example of such application is the use of the maximum average instantaneous overtopping discharge in a study on the stability of the inner slope of breakwaters (see Verhagen *et al.*, 2004).

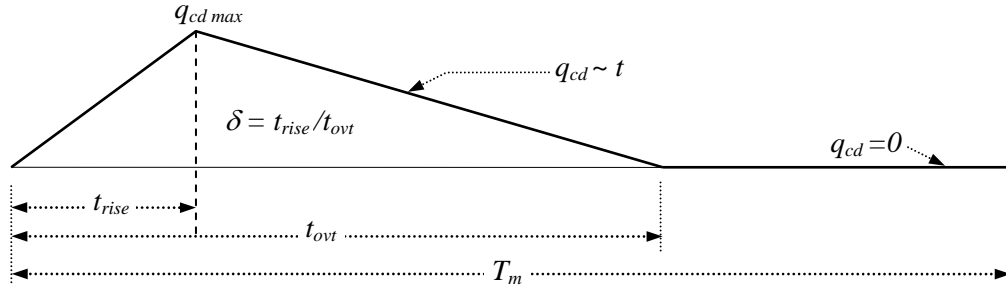


Figure 5 Average instantaneous overtopping discharge histogram.

4 Parameterization of wave overtopping

In this section we first discuss the derivation of the new slope definition used in the formulations of the key overtopping parameters. Next, the formulations of three primary parameters, i.e. the average overtopping discharge, the average overtopping time and the overtopping asymmetry are given. A sensitivity analysis of the data scattering for relevant parameters is then followed to evaluate the effectiveness of the new slope definition.

4.1 New definition of the equivalent slope and the tuning parameter

In an earlier study, Tuan [2003] derived a general simple equation defining the equivalent slope for sandy beaches, in which the upper and lower slopes together with the relative crest freeboard are variables. It was later found that that definition is too general and needs to be specified further to explicitly include the effect of the wave period. Also, to facilitate the verification of the new approach, an additional parameter (a tuning factor as shown in the following) is introduced. Following this direction, various modifications were tested to come up with a solution which is physically meaningful and mathematically correct. Eventually, a new form of the equivalent slope is given in the following:

$$m = m_s + \eta \frac{4m_b R_{cs}}{\xi_m H_{mo}} (m_b - m_s) \text{ with } \frac{R_{cs}}{H_{mo}} \leq 1. \quad (13)$$

Where m is the equivalent slope used in the overtopping calculation, m_s and m_b are the respective submerged (below water) and beach (dry) slopes, H_{mo} is the zeroth moment wave

height at the toe, ξ_m is the surf similarity parameter based on H_{m0} and the spectral period T_m , η is the slope tuning parameter.

The newly defined slope incorporates the effect of wave height and of the wave period. Its performance is discussed later in the analysis of the overtopping data, in which the parameter η is tuned to minimize scattering.

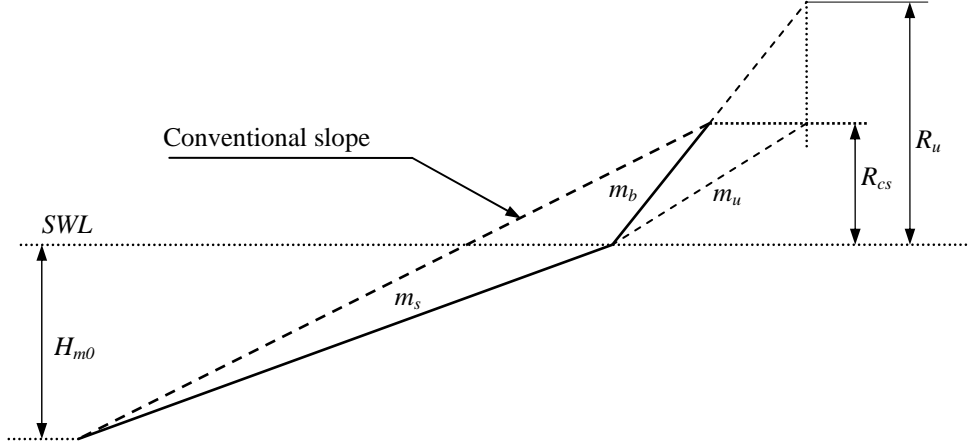


Figure 6. New approach of defining the equivalent slope.

The physical interpretation for this approach can be discerned from Fig. 6 and the following Eq. (14). Due to the crest shortage, run-up is cut off as waves reach the upper edge of the slope. Therefore, according to the definition of Van der Meer (see Van der Meer *et al.*, 1995; Van der Meer, 1998), hereinafter designated as the conventional approach, seen as the dashed line in Fig. 6, this cutoff makes no difference in sloping amongst waves with the same height but various wave periods as long as they overtop the slope. In the new approach, instead, longer waves “sense” gentler slopes as they run over.

Equation (13) can be rewritten as follows:

$$m = m_s + \eta' \frac{R_{cs}}{R_u / m_b} (m_b - m_s) = m_s + \eta' (m_b - m_s) m_u = m_s + \eta'' m_u. \quad (14)$$

Where, R_u is the fictitious run-up height, $R_u \sim \xi_m H_{m0}$.

$$m_u \text{ is the upper slope sensed by waves, } m_u = \frac{R_{cs}}{R_u / m_b} \text{ (see Fig. 6).}$$

In order to investigate the range of validity for the tuning parameter η , a maximum possible

value for the equivalent slope in Eq. (13) is considered, viz. when it equals the beach slope m_b :

$$m = m_s + \eta \frac{4m_b R_{cs}}{\xi_m H_{m0}} (m_b - m_s) \leq m_b.$$

$$\text{or } \eta \frac{4m_b R_{cs}}{\xi_m H_{m0}} \leq 1.0. \quad (15)$$

Substituting $\xi_m = \frac{m}{\sqrt{s_m}}$ into Eq. (15), yields:

$$\eta_{\max} = 1/4 \times 1 / \left(\frac{R_{cs}}{H_{m0}} \right)_{\max} \times 1 / \left(\frac{m_b}{m} \right)_{\max} \times 1 / \sqrt{(s_m)_{\max}}. \quad (16)$$

Where s_m is the fictitious wave steepness $s_m = \frac{2\pi}{g} \frac{H_{m0}}{T_m^2}$.

In Eq. (16), the ratio $\left(\frac{m_b}{m} \right) \rightarrow \max$ if $m = m_s$, but this only occurs when $m_b = m_s$. Thus,

$\left(\frac{m_b}{m} \right)_{\max} = 1$. In addition, taking $\left(\frac{R_{cs}}{H_{m0}} \right)_{\max} = 1$ and $(s_m)_{\max} = 0.06$ gives $\eta_{\max} \approx 1.0$.

Theoretically, the slope tuning parameter η lies in the range between 0 and 1 ($0 \leq \eta \leq 1$). On typical natural beach barriers, i.e. slopes with a gentle foreshore and without a dune scarp, the contribution from the submerged part seems exaggerated in a physical sense. Therefore, the most likely value of the parameter for the considered cases is between 0 and 0.50.

In the following section, it is shown that the above theoretical range can be further narrowed via a minimization of the scattering of the key overtopping parameters.

Since ξ_m is also a function of the equivalent slope, Eq. (13) is a quadratic equation with respect to this variable. Solving this equation gives the explicit expression of this slope according to:

$$m = \frac{1}{2} m_s + \frac{1}{2} \sqrt{m_s^2 + 16\eta m_b \frac{R_{cs}}{H_{m0}} \sqrt{s_m} (m_b - m_s)}. \quad (17)$$

For sake of comparison, the equivalent slope according to the conventional definition (Van der Meer, 1998) can also be derived from Fig. 6:

$$m = \frac{R_{cs} + 1.0H_{mo}}{1.0H_{mo}/m_s + R_{cs}/m_b}. \quad (18)$$

Equation (18) presents the principle of the two-point method (see Tuan, 2003), in which a composite slope is represented by a uniform equivalent slope within a pair of boundary points.

It is worth noticing, by definition, that the new equivalent slope defined by Eq. (13) or Eq. (17) is bounded by the upper beach slope m_b . Also, it is realized that, with waves of the same height but different periods, the conventional definition (Eq. (18)) always gives a fixed value of the equivalent slope whereas the new definition (Eq. (17)) produces slopes varied between m_s and m_b , depending on also the wave periods.

4.2 *The optimal wave period*

Different characteristic wave periods such as $T_{m0.1}$, $T_{m0.2}$, $T_{m-1.0}$, and T_P have been widely used in formulations of wave run-up and overtopping. Choices of one of these wave periods are also various, depending upon particular purposes. The definition for those periods based on spectral moments is given in Eq. (19).

$$T_{m\alpha.\beta} = \left(\frac{m_\alpha}{m_\beta} \right)^{\frac{1}{\beta-\alpha}} = \left(\frac{\int_0^\infty f^\alpha S(f) df}{\int_0^\infty f^\beta S(f) df} \right)^{\frac{1}{\beta-\alpha}}. \quad (19)$$

Where m_α and m_β stand for the wave spectral moments, α and β are integers.

A numerical study by Van Gent [2001] suggests to use the spectral period $T_{m-1.0}$ in describing wave run-up and wave overtopping for optimal results in cases of shallow foreshores, where wave spectra are flattened out. This conclusion is experimentally reconfirmed in the present study.

To evaluate the goodness-of-fit of data around a trend line or a prediction curve, a root-mean-square of the relative deviations between the measurement and the computed trend or prediction

was used. This is known as the scattering coefficient (Eq. (20)), of which a smaller value implies a better fit.

$$\varepsilon = \sqrt{\frac{1}{N_p} \sum_{i=1}^{N_p} \left(\frac{Y_{i,computed}}{Y_{i,measured}} - 1 \right)^2}. \quad (20)$$

Where Y is the considered dependent parameter, and N_p is the number of data points.

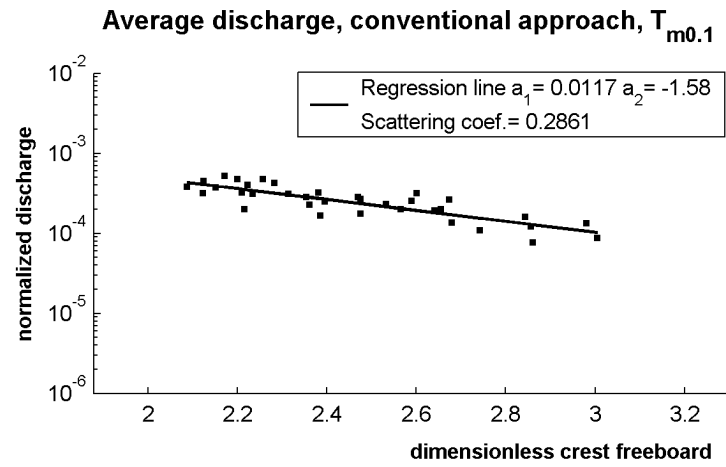
For sake of simplicity and without loss of generality, the default slope definition was used to analyze the overtopping data using different characteristic wave periods e.g. $T_{m0.1}$, $T_{m0.2}$, T_p , and $T_{m-1.0}$. Fig. 7 clearly shows that $T_{m-1.0}$ gives the least scattering ($\varepsilon = 0.147$), whereas the peak period T_p gives the largest scattering ($\varepsilon = 0.467$).

Hereinafter, this optimal spectral period $T_{m-1.0}$ is consistently used and denoted as T_m in the parameterization of wave overtopping.

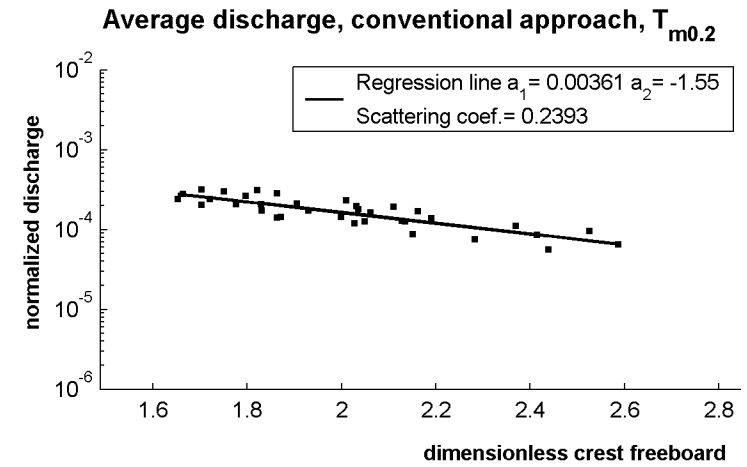
4.3 Formulations of overtopping parameters and effectiveness of the new slope definition

The average overtopping discharge, the average overtopping time and the overtopping asymmetry are three primary parameters which we seek to formulate directly from the experimental data as functions of the hydraulic conditions and the barrier geometry (see subsections 4.3.1 through 4.3.3). Other parameters such as the relative total overtopping time and the average instantaneous discharge can straightforwardly be deduced from these primary parameters.

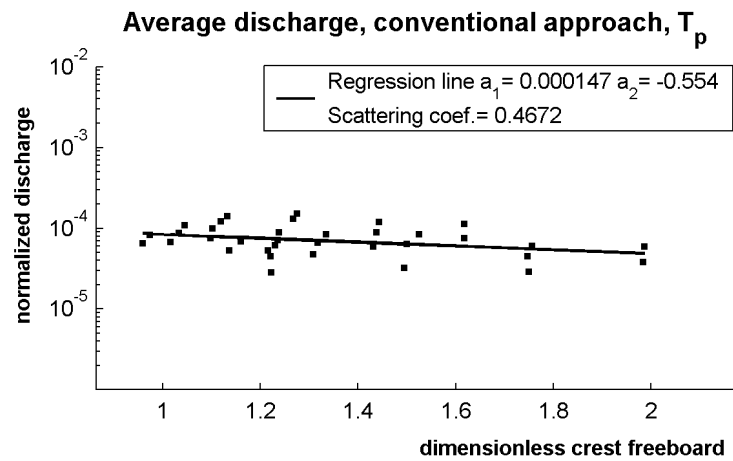
In order to explore the effectiveness of the new approach defining the equivalent slope, a sensitivity analysis of the data scattering for relevant parameters is carried out. This is done by tuning η in Eq. (13) within its range of validity (between 0 and 1) and inspecting the goodness-of-fit (scattering coefficient ε defined in Eq. (20)) of the overtopping data. A relationship between the scattering coefficient ε and η ($\varepsilon \sim \eta$) is therefore numerically established for each of the considered parameters. For sake of comparison, the data scattering associated with the slope defined by the conventional definition is also plotted (a constant value for each parameter). By



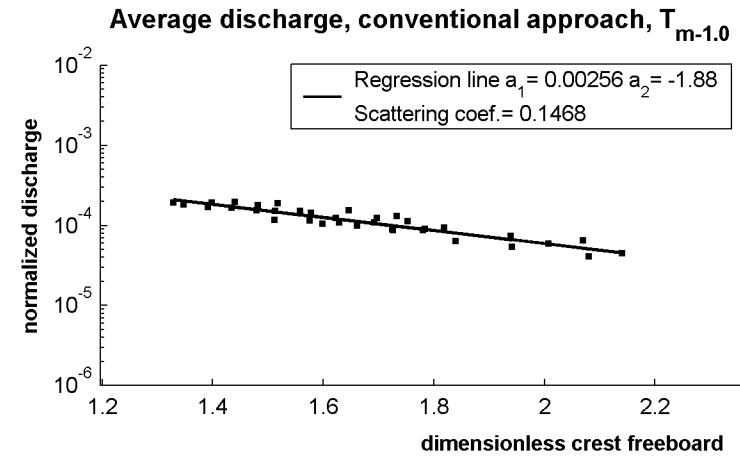
a- $T_{m0.1}$, $\epsilon = 0.286$



b- $T_{m0.2}$, $\epsilon = 0.239$



c- T_p , $\epsilon = 0.467$



d- $T_{m-1.0}$, $\epsilon = 0.147$

Figure 7. Normalized average overtopping discharge graphs with different characteristic periods: a- $T_{m0.1}$, b- $T_{m0.2}$, c- T_p , d- $T_{m-1.0}$.

doing so, a favorable range of the tuning parameter η is sought that fits the overtopping data the best. The average discharge and the wave-averaged overtopping time are the two reference parameters for this purpose. Tuning is not necessary, as shown later, for the overtopping asymmetry because already good fit is achieved using the conventional slope definition.

4.3.1 Average overtopping discharge

Adopting a slightly modified form as in Van der Meer [1998], the function describing the average overtopping discharge reads:

$$\frac{q}{\sqrt{gH_{mo}^3}} \frac{s_m}{\sqrt{\tan \alpha}} = a_1 \exp\left(a_2 \frac{R_{cs}}{H_{mo}} \frac{\sqrt{s_m}}{\tan \alpha}\right). \quad (21)$$

Where $\tan \alpha = m$ is the equivalent slope either according to the conventional or the new method.

Coefficients a_1 and a_2 are to be determined by means of a least square minimization procedure.

The modification of Eq. (21) compared to Van der Meer [1998] concerns the term s_m instead of $\sqrt{s_m}$ on the left hand side. This modification is based on various combination modes to give the best possible degree of regression in the current analysis.

The scattering relation $\varepsilon \sim \eta$ for the average overtopping discharge is shown as the upper curve in Fig.8. The conventional approach gives a fixed value of scattering $\varepsilon = 0.147$ (see also Fig. 7d). In comparison with the new approach, it follows that the conventional method introduces larger scattering over a wide range of η between 0 and 0.90. The optimal value of η , corresponding with the least scattering, is 0.19.

Figure 9a shows the result for the average discharge data plotted at the point of least scattering.

4.3.2 Wave-averaged overtopping time

Apart from being a function of the dimensionless crest-freeboard and the surf similarity parameter (just like the average discharge), the average overtopping time t_{ovt} is also dependent on the relative total overtopping time F_{cd} as shown in Eq. (7). The optimal dimensionless form

quantifying t_{ovt} is shown in Eq. (22), also based on investigating various modes of parameter combinations to yield the best degree of regression (the least scattering coefficient).

$$\frac{t_{ovt}}{T_m} \sqrt{\frac{s_m}{\tan \alpha}} = F_{cd} \sqrt{\frac{s_m}{\tan \alpha}} = a_1 \exp \left(a_2 \frac{\sqrt{s_m}}{\tan \alpha} \left(\frac{R_{cs}}{H_{mo}} \right)^{3/2} \right). \quad (22)$$

The lower curve in Fig. 8 shows the relation $\varepsilon \sim \eta$ for the wave-averaged overtopping time. The scattering resulted from the conventional slope definition is 0.09 (see Fig. 9c). In this case, the new approach indicates a better regression over the entire range of the tuning parameter. The least scattering is achieved at the optimal value $\eta = 0.35$. The result for the wave-averaged overtopping time at the point of least scattering is shown in Fig. 9b.

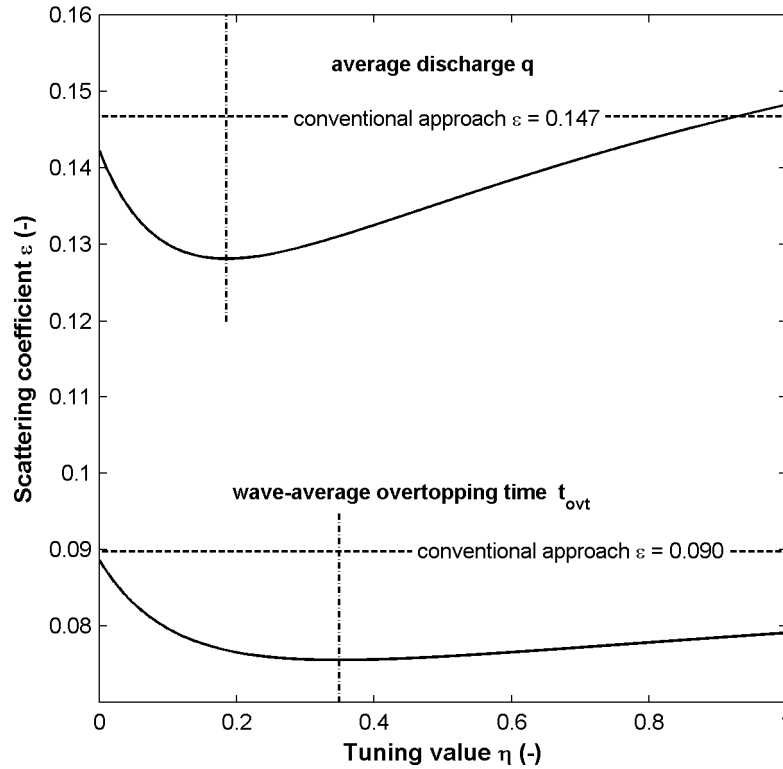


Figure 8. Relation $\varepsilon \sim \eta$ for the average discharge (upper) and the wave-averaged overtopping time (lower).

4.3.3 Overtopping asymmetry

Following the same procedure as for the two previous parameters, the overall asymmetry of overtopping triangles and also the discharge histogram is characterized by the following

dimensionless expression:

$$\delta \sqrt{\frac{s_m}{\tan \alpha}} = a_1 \left(\frac{\tan \alpha}{\sqrt{s_m}} \frac{R_{cs}}{H_{mo}} \right)^{a_2}. \quad (23)$$

Figure 9c shows the result for the overtopping asymmetry using the conventional slope definition. It is observed that the data are very well fitted without tuning necessity.

4.3.4 Overall effectiveness of the new equivalent slope and the favorable range of η

As mentioned above, the relations $\varepsilon \sim \eta$ have been established from the experimental data for both the average discharge and the wave-averaged overtopping time as in Fig. 8. Overall, the new approach clearly shows its advantage over the conventional one nearly over the entire theoretical range of the tuning parameter. Even so, it does not come up with a single best value of the tuning parameter since its optimal values for the two reference parameters are not coincident. However, the most concave portions of the both curves in Fig. 8 lie between 0.10 and 0.40 on the η -axis, which is also in agreement with the range that is likely to occur in the field mentioned earlier. This would be a compromising range ($\eta=0.1\sim 0.4$) if one desires to optimize the tuning with both of the reference parameters.

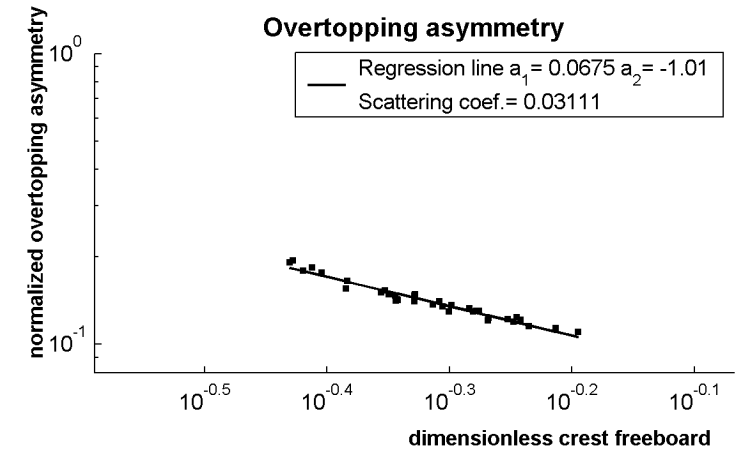
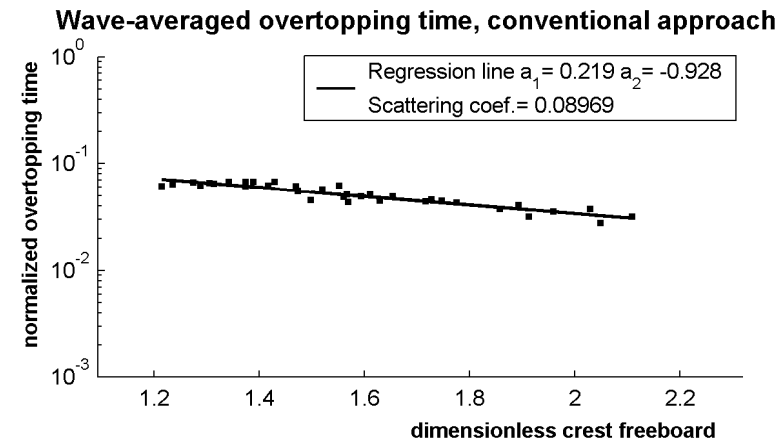
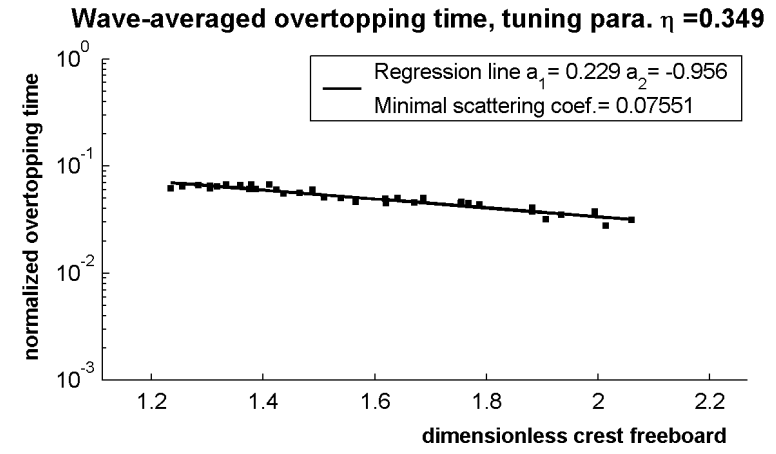
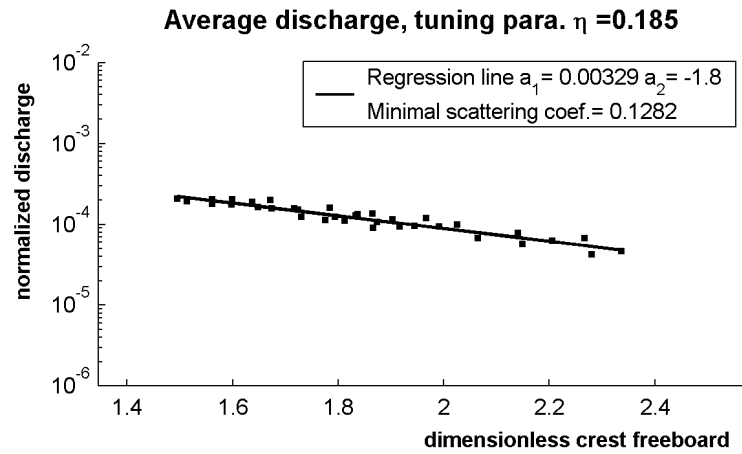


Figure 9. Normalized graphs of the primary overtopping parameters.
(Data associated with the new slope definition are plotted at the point of least scattering)

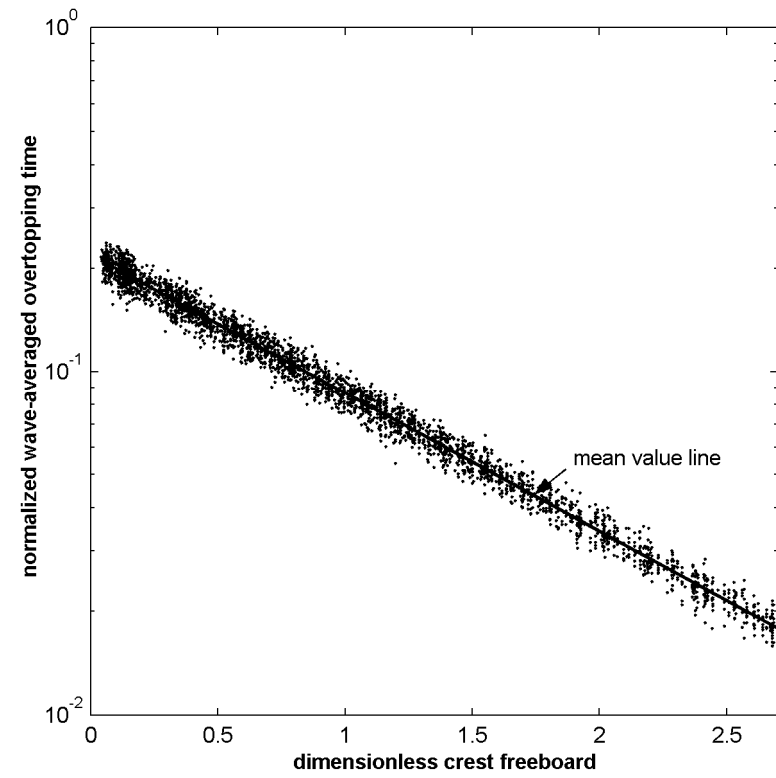
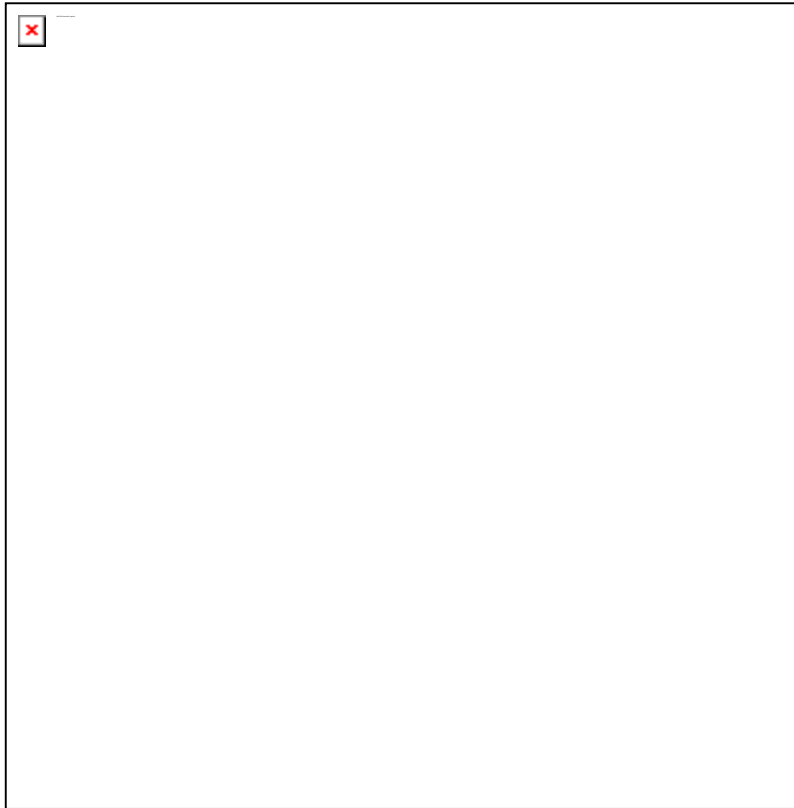


Figure 10. Randomly generated overtopping data (normal distribution) $N = 3150$ points.

4.4 Numerical optimization of η

We conclude that there exists no single optimal value of the slope tuning parameter, which can simultaneously assure the least scattering of the two reference parameters. However, a favorable range that captures a satisfactory goodness-of-fit can be obtained. We further note that, it is arguable, on mathematical grounds, that a considered quantity (discharge or overtopping time) is in fact a function of geometric conditions (slope steepness and freeboard) and of hydraulic parameters, in which η is an implicit variable. Thereby, the data scattering and the number of data points may affect the optimization of η . With a given measurement error, which is presumed to be the same for all the tests (the same scattering), then the number of data points might be the most influential. It is shown in the following how numerical experiments can be utilized to study this issue. The approach is to generate new datasets to obtain a sufficiently large number of data points over a wide range covering the domain of interest, based on the stochastic properties of the existing experimental data. In this way, new data points of the dimensionless overtopping parameters are randomly generated on the assumption that they obey a normal distribution characterized by mean values and standard deviations (scatterings). To investigate the effect of the data scattering on the optimization of η , different values of the standard deviation coefficients ν (standard deviation divided by a mean) are assumed for the analysis including those obtained from the measurement data (0.147 and 0.09 for the average discharge and the wave-averaged overtopping time, respectively, cf. Figs. 7d and 9c).

The wave data from 35 laboratory tests (Table 1) are used to form the basic hydraulic input since they cover a wide range of wave conditions on shallow foreshores. In detail, the mean values of the reference parameters are respectively determined by Eqs. (21) and (22), using the conventional slope definition and the corresponding regression coefficients from the laboratory experiment (0.0026 and -1.88 for Eq. (21), 0.219 and -0.928 for Eq. (22), cf. Figs. 7d and 9c).

The crest freeboard and the slope steepness reflect the two geometric conditions of the barrier. In this numerical experiment, the relative crest freeboard ($R_{cs}/H_{mo,toe}$) is varied over its full range

between 0 and 1. A wide range of typical beach slopes from 1/30 to 1/5 is also selected to constitute a number of sets of the composite profile.

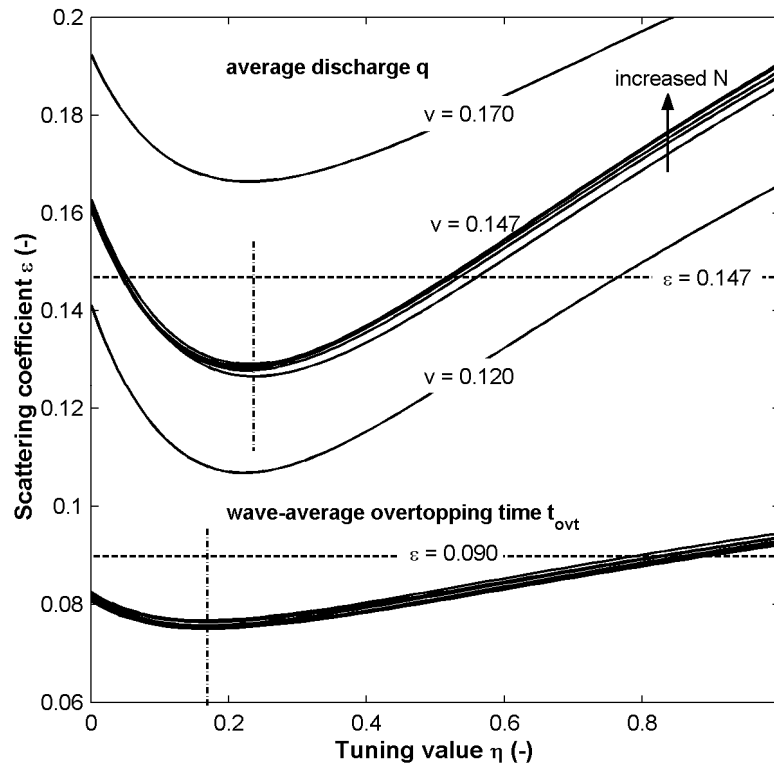


Figure 11. Relation $\varepsilon \sim \eta$ of the randomly generated overtopping data: effects of scattering and number of data points. Upper graph - the average discharge with different degrees of scattering (scattering coefficient $v=0.12\sim 0.17$). Lower graph - the wave-averaged overtopping time.

In total, one hydraulic and two geometric conditions form a three-dimension matrix of data points. The size of each matrix dimension can be varied according to the number of data points needed. Figures 10a and 10b show the result of a generation of 3150 data points ($35 \times 18 \times 5$) for the average discharge and the wave-averaged overtopping time, respectively. The newly-generated data points are then used for the tuning as is done in section 4.3. The results from the tuning as shown in Fig. 11 indicate that the generation randomness may affect the shape of the ($\eta \sim \varepsilon$) curves if the number of data points N is insufficiently large. The curves become stable at $N > 3000$ points. Interestingly, it also follows that the optimization of η is indeed most influenced by the number of data points covering the domain of interest. The position of the peaks of the two curves on the horizontal axis is not sensitive to the change in the data scattering, which is reflected by different values of v . On the whole, the two peaks do not

coincide precisely on the η -axis but are quite close. The optimal tuning value is now in the range between 0.15 and 0.25 that is appreciably narrower than the one deduced from the laboratory data.

Table 2. Regression coefficients.

Tuning η	Average discharge (Eq. (21))		Overtopping time (Eq. (22))	
	a_1	a_2	a_1	a_2
0.10	0.0033	-1.67	0.250	-0.804
0.15	0.0033	-1.75	0.245	-0.840
0.20	0.0033	-1.83	0.241	-0.873
0.25	0.0033	-1.90	0.236	-0.903
0.30	0.0032	-1.96	0.232	-0.930
0.35	0.0032	-2.02	0.229	-0.957
0.40	0.0032	-2.08	0.225	-0.982
0.45	0.0031	-2.13	0.222	-1.010
0.50	0.0031	-2.18	0.219	-1.030

Note: the grey area corresponds to the most favorable range of the slope tuning parameter

4.5 Final formulations

With the above optimal range of η between 0.15 and 0.25, the following Table 2 is elaborated for each pairs of regression coefficients in Eq. (21) and Eq. (22). Equally, these coefficients can be determined as functions of the tuning parameter as follows:

Discharge equation (Eq. (21)):

$$a_1 = 0.0034 - 0.0006\eta \quad a_2 = -1.64 - \eta \quad (24a)$$

Overtopping time equation (Eq. (22)):

$$a_1 = 0.255 - 0.07\eta \quad a_2 = -0.788 - 0.45\eta \quad (24b)$$

The coefficients in Eq. (23) are 0.0675 and approximate -1.0, with the equivalent slope determined using either the conventional approach or the new method since the tuning effect is less sensitive in this case (no significant difference in regression). Eq. (23) therefore can be rewritten in the following form:

$$\delta = \frac{0.0675}{\sqrt{\tan \alpha}} \frac{1}{R_{cs} / H_{mo}}. \quad (25)$$

Coefficients from Eqs. (24a) and (24b) are used to determine the average discharge and the relative total overtopping time according to Eqs. (21) and (22), respectively. The average instantaneous discharge is then fully determined using Eq. (9) to Eq. (12).

5 Discussion of results

In the foregoing sections, key parameters from breakwater overtopping literature were modified to describe the nature of overtopping on beach barriers in conjunction with an improved definition of the equivalent slope. Our aim is to improve the description of wave overtopping discharge for use in numerical modeling of wave overwash. In general, the research results are conceptually adoptable to other practical engineering applications. However, certain aspects involving the use of the findings need to be addressed:

(1) It is technically impossible to generate data from mobile bed (sand) experiments to verify the new slope approach and the formulation of the key overtopping parameters. In the case of a mobile bed, the slope variation and the bed roughness are major factors which may differ overtopping discharge calculation from that of a fixed bed. However, it is shown in the following that possible deviations induced by those two factors can be exempted and the current findings from the fixed-bed experiment are therefore transferable to movable (sand) beds.

First, within a computation time step of one to several wave cycles, the profile evolution of a movable bed is negligibly small and thus the bed may be considered instantaneously fixed. Moreover, the assumption of quasi-steadiness, which is widely accepted for various purposes of numerical modeling, allows the instantaneous overtopping parameters to be related to the instantaneous (through the wave-cycle) slope geometry and incident wave parameters. As a result, effects of the slope variation in the quantification of wave overtopping discharge can be neglected.

Second, as already mentioned in section 2, the model slopes were made smooth to fulfill a proper scaling for wave overtopping. This is because wave runup and overtopping on sloping

impermeable structures can be underestimated in model tests due to the inability to scale roughness effects. This is also true for the current situation where the prototype is a mobile (sandy) slope. However, this scale effect, in principle, can be minimized by making model slopes very smooth (see Hughes, 1993, p.215). Also, fixed-bed model tests with smooth slopes are commonly used for studying wave interactions on natural beaches such as wave runup by Battjes [1974], Mayer and Kriebel [1994].

(2) By definition, the new approach for defining the equivalent slope is generally valid for any low-crested (with occurrence of wave overtopping, quantitatively $R_{cs}/H_{mo} \leq 1$) profiles and wave steepness between 0.01 and 0.06. Consequently, the tuning parameter theoretically lies between 0 and 1.

It is worth noticing that, as the scope of the present work, the approach was not tested with steep slopes (say larger 1/6, see also Mayer and Kriebel, 1994) rather than with those of typical many natural beaches. Likewise, the conditions of deep foreshores have not been considered. The validity of this new approach therefore falls under the conditions of sandy beaches with shallow foreshores. Nevertheless, it does not mean that the approach has a limited application. In fact, a large number of natural sea-defence works (dunes and barriers for instance) found on gently sloping shallow parts of the coast, namely shallow foreshores, where the beach profile exhibits complexity due to high activities of depth-induced wave breaking. On those beaches, the definition of the equivalent slope is a real dilemma and the new approach is an eligible solution.

(3) The newly-defined parameters were formulated using the experimental data of wave overtopping at impermeable and smooth slopes. Effects of slope roughness and porosity therefore must be taken into consideration in cases of high permeability and friction such as rock and gravel slopes.

(4) Because the slope tuning parameter is implicitly depending on the overtopping formulations, its value range and the associated regression coefficients (Table 2 or Eq. (24)) actually create an additional flexibility for other calibration purposes. For this reason, in the next step of the current research, it is preferable that the final choice of this parameter within the favorable range

will be specified further according to morphological considerations. For the unique purpose of overtopping calculation a tuning value of $\eta = 0.20$ is recommended.

6 Summary and conclusions

Laboratory experiments were carried out to increase insight into the hydraulic characteristics of wave overwash on smooth slopes and low-crested barriers on shallow foreshores. Our final goal is to describe wave overtopping discharge as an event-based approach i.e. describing its discontinuous and temporal behaviors through the wave cycle. This elaboration is necessary for the purpose of numerical modeling of morphological changes due to wave overwash where the use of an average overtopping discharge is inadequate. For this purpose, several new parameters such as the wave-averaged overtopping time, the overtopping asymmetry, the relative total overtopping time, the average maximum discharge and the average instantaneous discharge have been derived including a new slope definition.

The new definition of the equivalent slope effectively takes into account effects of the wave period, which become significant when large variations in the relative crest freeboard and in slopes are present. The efficiency of the new slope definition is enhanced via the use of the slope tuning parameter η , whose favorable values have been experimentally found in the range between 0.10 and 0.40. This range has been further narrowed to between 0.15 and 0.25 by means of a numerical experiment. Hence, the tuning value of $\eta = 0.2$ would be recommended for overtopping estimates. However, for applications where the ultimate goals are not only the overtopping quantities, it is recommended to further calibrate this parameter (within its indicated range) according to additional corresponding criteria.

For use in the empirical determination of wave overtopping discharge, the experimental results suggest that the ordinary slope definition such as by Van der Meer [1998] is most suitable for hard structures where the crest freeboards are relatively constant and slopes are relatively uniform. However, on natural sandy beaches the profile is complex and can markedly change during wave attack. Therefore, the equivalent slope defined by the new approach is more

appropriate. The results also assert on the use of the spectral period $T_{m-1.0}$ for an optimal description of wave overtopping at beaches on shallow foreshores.

Acknowledgements

The authors acknowledge the financial support via the co-operational project funded by the Royal Netherlands Embassy in Hanoi in Coastal Engineering between Delft University of Technology and Hanoi Water Resources University. The constructive and valuable comments of the reviewers are gratefully appreciated.

References

- Battjes, J.A. (1974). Surf similarity. *Proc. 14th Coast. Engrg. Conf.*, 466-480.
- Hughes, A.S. (1993). Physical models and laboratory techniques in coastal engineering. *World Scientific, Singapore*, 568 pp.
- Latherman, S.P. (Ed.). (1981). Overwash processes. *Benchmark paper in geology. Hutchinson Ross Pub. Co., Stroudsburg, PA*, 58 , 376 pp.
- Mayer, R.H. and Kriebel, D.L. (1994). Wave runup on composite slope and concave beaches. *Proc. 24th Coast. Engrg. Conf., ASCE*, 2325-2339.
- Kobayashi, N., Tega, Y. and Hancock, M.W. (1996). Wave reflection and overwash of dunes. *J. Wtrway. Port, Coast. Oc. Engrg., ASCE*, 122(3), 150-153.
- Tega, Y. and Kobayashi, N. (1999). Numerical modeling of over-washed dune profiles. *Coastal Sediment'99, ASCE*, 1355-1369.
- Tuan, T. Q. (2003). Time-varying equivalent slope for overwash models in simulation of lagoon initial breaching (on CD). *Proc. COPEDEC VI, Colombo, 2003*. Paper No. 089.
- Van der Meer, J.W., Janssen, J.P.F.M. (1995). Wave run-up and wave overtopping at dikes. In: *Kobayashi, N., Demirbilek, Z.(Eds.), Wave Forces on Inclined and Vertical Structures*, ASCE, 1-26.
- Van der Meer, J.W. (1998). Wave run-up and overtopping. In: *Dikes and Revetments: Design*,

Maintenance and Safety Assessment, Pilarczyk, K.W. (Ed.), A.A.Balkema, Rotterdam, The Netherlands, 1998, 145-159.

Van Gent, M.R.A. (2001). Wave run-up on dikes with shallow foreshores. *J. Waterway, Port, Coast. Oc. Engrg., ASCE*, 127(5), 254 -262.

Verhagen, H.J., Steenaard, J., Tuan, T.Q. (2004). Infiltration of overtopping water in a breakwater crest. *Proc. 29th Coast. Engrg. Conf.*, Lisbon, Portugal.